

Ketchikan, Alaska LiDAR & Digital Imagery

Technical Data Report



STARR

Stantec, Inc., attn: James Huffines
5565 Centerview Drive, Suite 107
Raleigh, NC 27606
PH: 919-532-2332



Project No. 4140618
QSI Anchorage Office
2014 Merrill Field Drive
Anchorage, AK 99501
PH: 907-272-4495

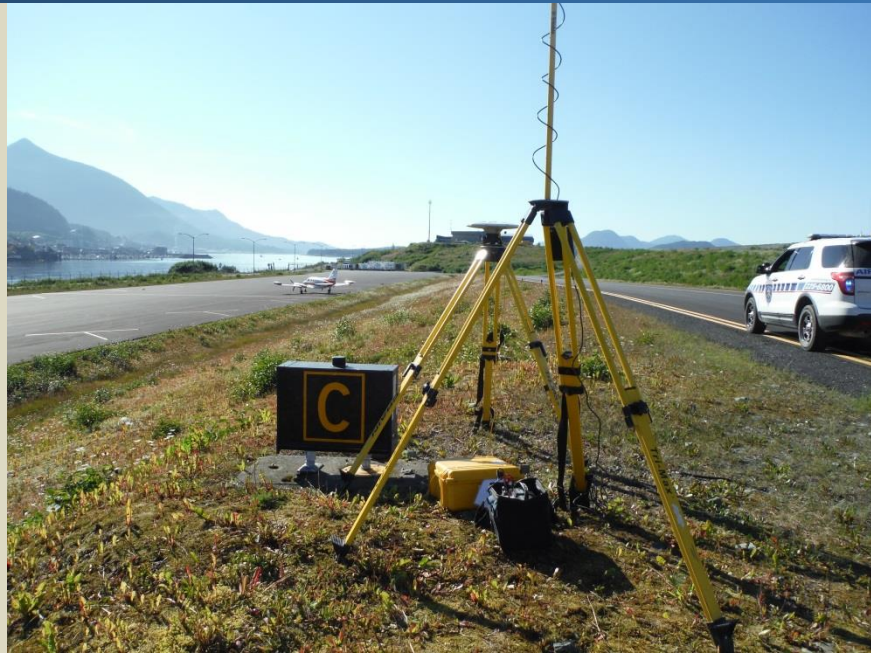
TABLE OF CONTENTS

INTRODUCTION	1
Deliverable Products	2
ACQUISITION	4
Pre- Flight Operations Planning	4
Ground Survey.....	5
Monumentation	5
Ground Survey Points (GSPs).....	6
Airborne Survey.....	9
LiDAR.....	9
Digital Imagery.....	10
PROCESSING	11
LiDAR Data.....	11
Feature Extraction	13
Contours	13
Digital Imagery	14
RESULTS & DISCUSSION	15
LiDAR Density	15
LiDAR Accuracy Assessments	18
LiDAR Absolute Accuracy.....	18
LiDAR Supplemental and Consolidated Vertical Accuracies.....	19
Digital Imagery Accuracy Assessment.....	20
CERTIFICATIONS	23
SELECTED IMAGES.....	24
GLOSSARY	28
APPENDIX A - ACCURACY CONTROLS	29
LiDAR Supplemental Vertical Accuracies.....	30
GPS Separation and Altitude Plots, PDOP Plots	32
07/12/2014.....	32
07/13/2014.....	34

Cover Photo: A view looking north/northeast over an inlet on the north shore of Gravina Island. The image was created from the gridded LiDAR surface colored by elevation and overlaid with 2 foot contours and the LiDAR point cloud.

INTRODUCTION

This photo taken by QSI acquisition staff shows a view of ground survey equipment set up on site at the Ketchikan Airport.



In June 2014, Quantum Spatial (QSI) was contracted by the Strategic Alliance for Risk Reduction (STARR) to collect Light Detection and Ranging (LiDAR) data and digital imagery in the summer of 2014 for the Ketchikan site in Alaska. Data were collected to aid STARR in assessing the topographic and geophysical properties of the study area in order to perform flood risk assessment and mapping for the Federal Emergency Management Agency (FEMA).

This report accompanies the delivered LiDAR data and imagery, and documents contract specifications, data acquisition procedures, processing methods, and analysis of the final dataset including LiDAR and orthophoto accuracy. Acquisition dates and acreage are shown in Table 1, a complete list of contracted deliverables provided to STARR is shown in Table 2, and the project extent is shown in Figure 1.

Table 1: Acquisition dates, acreage, and data types collected on the Ketchikan site

Project Site	Contracted Acres	Buffered Acres	Acquisition Dates	Data Type
Ketchikan, Alaska	17,718	22,088	07/12/2014	LiDAR
			07/13/2014	
			07/12/2014	4 band (RGB-NIR) Digital Imagery

Deliverable Products

Table 2: Products delivered to STARR for the Ketchikan site

Ketchikan Products Projection: Alaska State Plane Zone 1 Horizontal Datum: NAD83 (2011) Vertical Datum: NAVD88 (GEOID12A) Units: US Survey Feet	
Points	LAS v 1.2 <ul style="list-style-type: none"> • All Returns • Flightline Swaths
Rasters	3.0 Foot ESRI Grids <ul style="list-style-type: none"> • Bare Earth Model • Highest Hit Model*
Vectors	Shapefiles (*.shp) <ul style="list-style-type: none"> • Site Boundary • LiDAR Tile Index • Orthoimagery Tile Index • Flightline Swath Index
Digital Imagery	0.3 Ft Pixel GeoTiffs (*.tif) <ul style="list-style-type: none"> • Imagery Mosaics (RGBN)

**QSI delivered these LiDAR derived products in addition to contracted deliverables in order to provide STARR with a more complete and versatile dataset.*

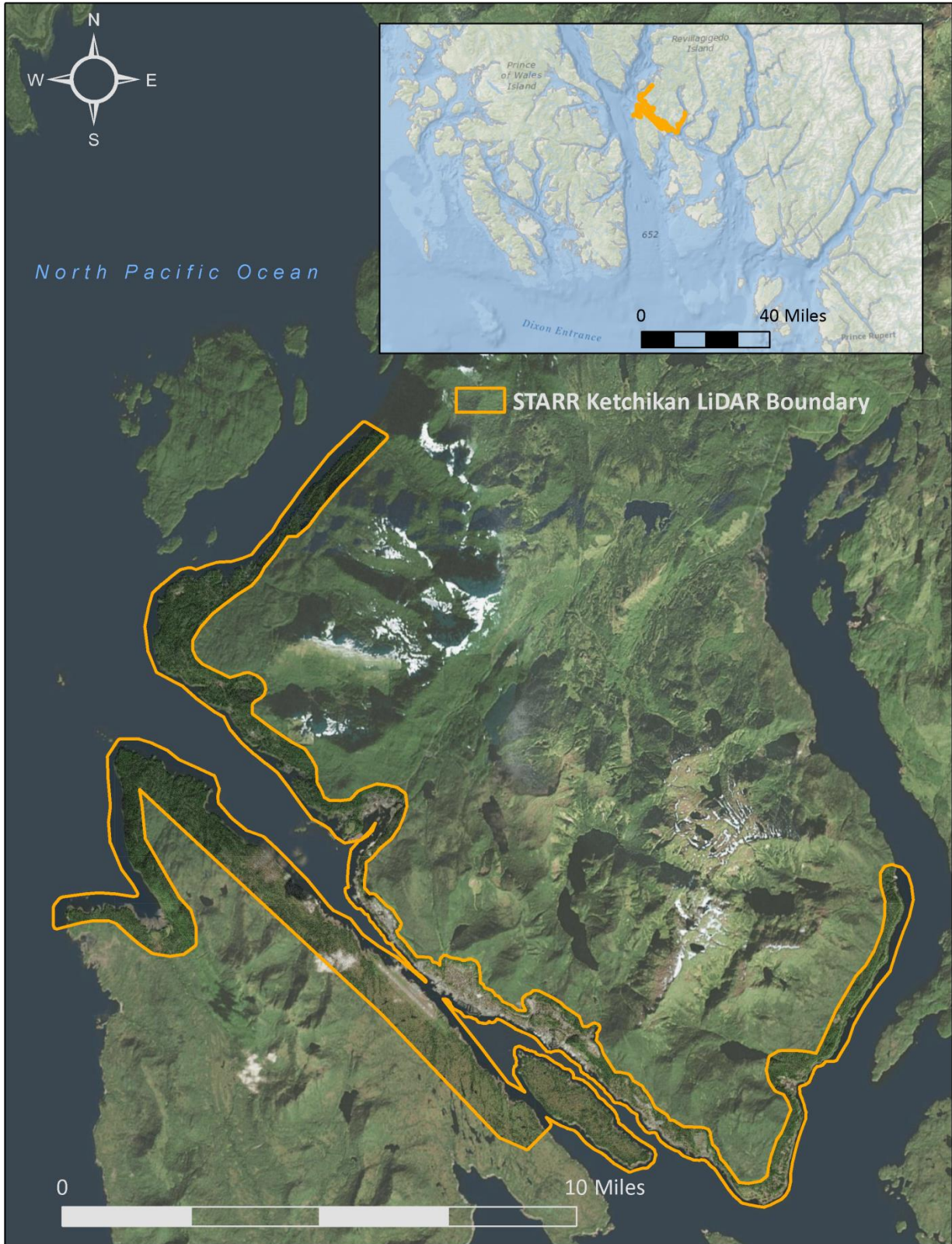


Figure 1: Location map of the Ketchikan site in Alaska

Quantum Spatial's Piper Navajo used in the STARR Ketchikan data acquisition



Pre- Flight Operations Planning

In preparation for data collection, QSI reviewed the project area and developed specialized flight plans to ensure complete coverage of the Ketchikan study area at the specified LiDAR point density of ≥ 4.0 points/m² (0.37 points/ft²) and specified orthophoto native pixel resolution of ≤ 30 cm. Acquisition parameters including orientation relative to terrain, flight altitude, pulse rate, scan angle, and ground speed were adapted to optimize flight paths and flight times while meeting all contract specifications.

Factors such as satellite constellation availability and weather windows must be considered during the planning stage. Any weather hazards or conditions affecting the flight were continuously monitored due to their potential impact on the daily success of airborne and ground operations. In addition, logistical considerations including private property access, potential air space restrictions, and tide conditions were reviewed (Figure 2).

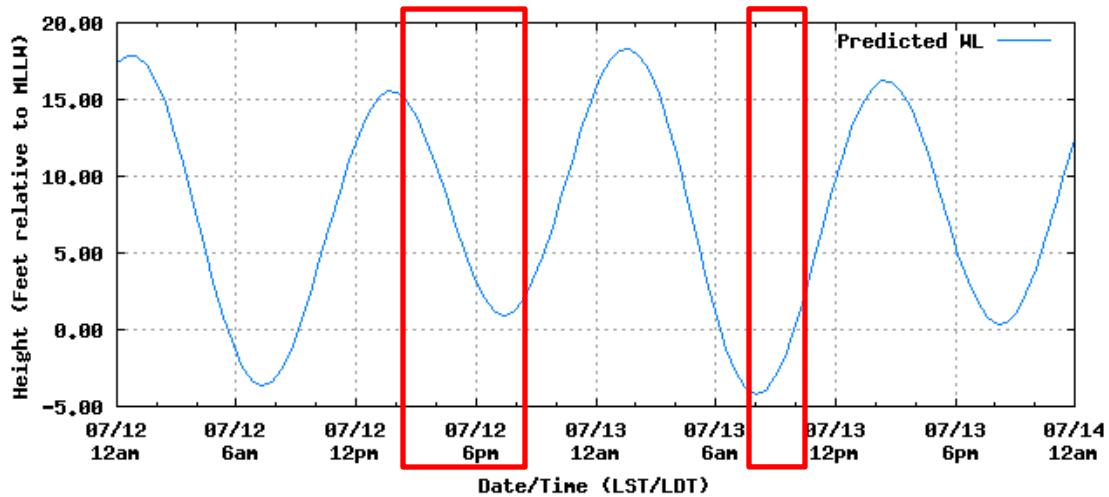


Figure 2: NOAA tide prediction chart for Ketchikan, Alaska, Station ID No. 9450460, at the time of LiDAR acquisition (July 12, 13, 2014). Planned flight times are outlined in red.

Ground Survey

Ground control surveys, including monumentation, aerial targets and ground survey points (GSPs), were conducted to support the airborne acquisition. Ground control data were used to geospatially correct the aircraft positional coordinate data and to perform quality assurance checks on final LiDAR data and orthoimagery products.

Monumentation

The spatial configuration of ground survey monuments provided redundant control within 13 nautical miles of the mission areas for LiDAR flights. Monuments were also used for collection of ground survey points using real time kinematic (RTK) survey techniques.

Monument locations were selected with consideration for satellite visibility, field crew safety, and optimal location for GSP coverage. QSI established one new monument and utilized one existing monument for the Ketchikan LiDAR project (Table 3, Figure 3). New monumentation was set using 5/8" x 30" rebar topped with stamped 2" aluminum caps. QSI's professional land surveyor, Evon Silvia oversaw the establishment and occupation of all monuments.



QSI-Established Monument



Existing Monument

Table 3: Monuments established for the Ketchikan acquisition. Coordinates are on the NAD83 (2011) datum, epoch 2010.00

Monument ID	Latitude	Longitude	Ellipsoid (meters)
KKN_01	55° 24' 37.17621"	-131° 43' 24.31649"	30.225
KTN4	55° 21' 15.49304"	-131° 42' 24.82915"	6.720

To correct the continuously recorded onboard measurements of the aircraft position, QSI concurrently conducted multiple static Global Navigation Satellite System (GNSS) ground surveys (1 Hz recording frequency) over each monument. During post-processing, the static GPS data were triangulated with nearby Continuously Operating Reference Stations (CORS) using the Online Positioning User Service (OPUS¹) for precise positioning. Multiple independent sessions over the same monument were processed to confirm antenna height measurements and to refine position accuracy.

¹ OPUS is a free service provided by the National Geodetic Survey to process corrected monument positions. <http://www.ngs.noaa.gov/OPUS>.

Monuments were established according to the national standard for geodetic control networks, as specified in the Federal Geographic Data Committee (FGDC) Geospatial Positioning Accuracy Standards for geodetic networks.² This standard provides guidelines for classification of monument quality at the 95% confidence interval as a basis for comparing the quality of one control network to another. The monument rating for this project is shown in Table 4.

Table 4: Federal Geographic Data Committee monument rating for network accuracy

Direction	Rating
1.96 * St Dev _{NE} :	0.020 m
1.96 * St Dev _z :	0.050 m

For the Ketchikan LiDAR project, the monument coordinates contributed no more than 5.4 cm of positional error to the geolocation of the final ground survey points and LiDAR, with 95% confidence.

Ground Survey Points (GSPs)

Ground survey points were collected using real time kinematic survey techniques. A Trimble R7 base unit was positioned at a nearby monument to broadcast a kinematic correction to a roving Trimble R10 GNSS receiver. All GSP measurements were made during periods with a Position Dilution of Precision (PDOP) of ≤ 3.0 with at least six satellites in view of the stationary and roving receivers. When collecting RTK data, the rover records data while stationary for five seconds, then calculates the pseudorange position using at least three one-second epochs. Relative errors for the position must be less than 1.5 cm horizontal and 2.0 cm vertical in order to be accepted. See Table 5 for Trimble unit specifications.

Table 5: Trimble equipment identification

Receiver Model	Antenna	OPUS Antenna ID	Use
Trimble R7 GNSS	Zephyr GNSS Geodetic Model 2	TRM57971.00	Static
Trimble R8	Integrated Antenna R8 Model 2	TRM_R8_GNSS	Static
Trimble R10	Integrated Antenna R10	TRMR10	Rover

² Federal Geographic Data Committee, Geospatial Positioning Accuracy Standards (FGDC-STD-007.2-1998). Part 2: Standards for Geodetic Networks, Table 2.1, page 2-3. <http://www.fgdc.gov/standards/projects/FGDC-standards-projects/accuracy/part2/chapter2>

LiDAR Ground Control Points

LiDAR ground control points, used during the calibration process, were collected in areas where good satellite visibility was achieved on paved roads and other hard surfaces such as gravel or packed dirt roads. Ground control point measurements were not taken on highly reflective surfaces such as center line stripes or lane markings on roads due to the increased noise seen in the laser returns over these surfaces. Ground control points were collected within as many flightlines as possible; however the distribution of ground control points depended on ground access constraints and monument locations and may not be equitably distributed throughout the study area (Figure 3).

LiDAR Land Cover Check Points

In addition to ground control points, land cover check points were collected throughout the study area. Land cover check points were not used during the calibration process and are used to calculate the vertical accuracy of the LiDAR dataset. Individual accuracies were calculated for each land cover type to assess confidence in the LiDAR derived ground models across land cover classes. Land cover types and descriptions are shown in Table 6.

Table 6: Land cover descriptions of check points taken for the Ketchikan site

Land cover type	Land cover code	Description
Evergreen Forest	EVER_FOR	Areas dominated by trees where 75 percent or more of the tree species maintain their leaves all year. Canopy is never without green foliage
Park/Urban/ Recreational Area	PARK/URBAN/REC	Includes areas with a mixture of constructed materials and vegetation.
Gravel	GVL	Perennially barren areas of bedrock, pavement, gravel, or other accumulations of earthen material.

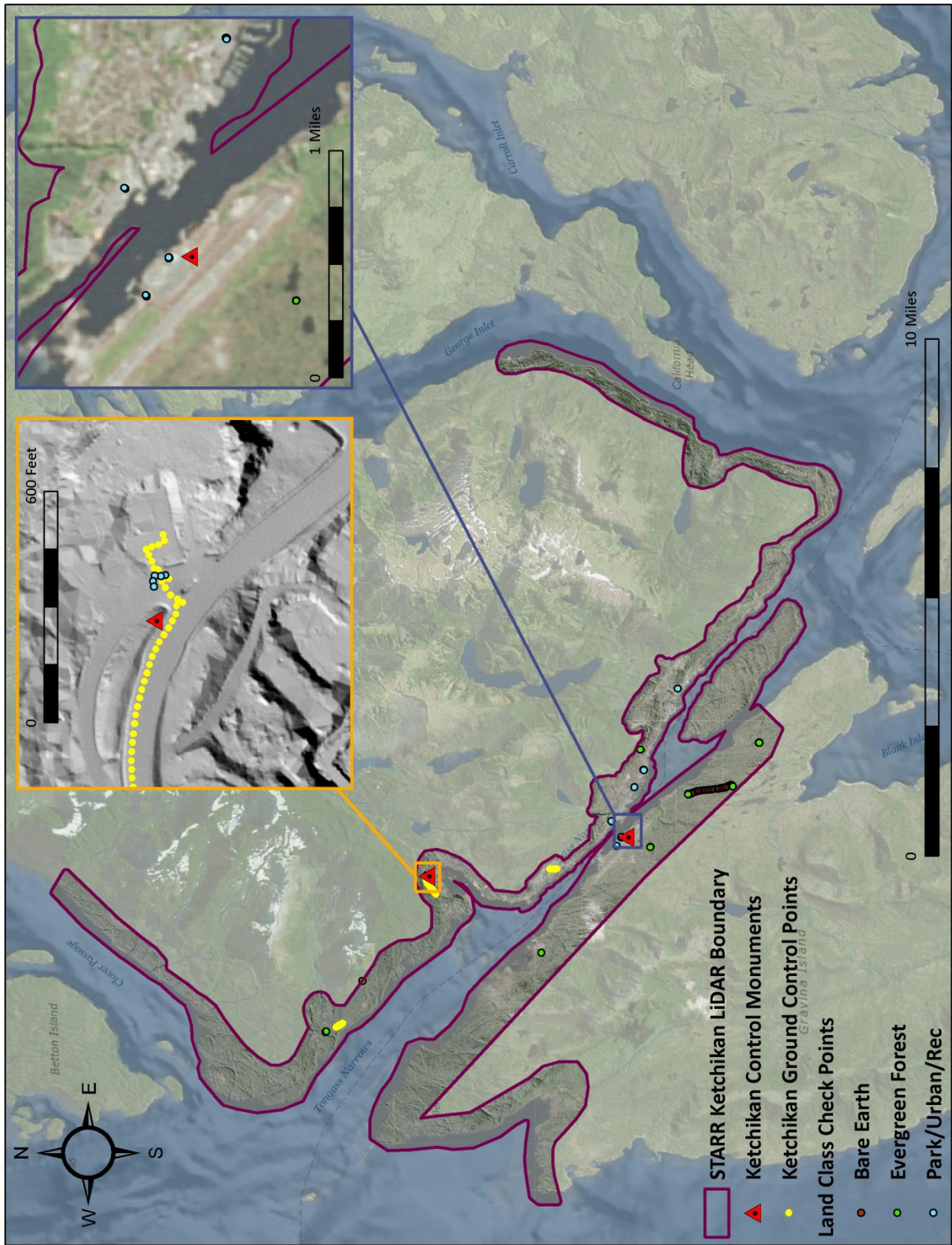


Figure 3: Ground control location map

Airborne Survey³

LiDAR

The LiDAR survey was accomplished using a Leica ALS70 system mounted in a Piper Navajo. Table 7 summarizes the settings used to yield an average pulse density of ≥ 4 pulses/m² over the Ketchikan project area. The Leica ALS70 laser system can record unlimited range measurements (returns) per pulse, but typically does not record more than 5 returns per pulse. It is not uncommon for some types of surfaces (e.g., dense vegetation or water) to return fewer pulses to the LiDAR sensor than the laser originally emitted. The discrepancy between first return and overall delivered density will vary depending on terrain, land cover, and the prevalence of water bodies. All discernible laser returns were processed for the output dataset.

Table 7: LiDAR specifications and survey settings

LiDAR Survey Settings & Specifications	
Acquisition Dates	July 12 - 13, 2014
Aircraft Used	Piper Navajo
Sensor	Leica ALS70
Survey Altitude (MSL)	5207 - 5315 ft
Target Pulse Rate	175 kHz
Pulse Mode	Single Pulse in Air (SPiA)
Laser Pulse Diameter	37 cm
Mirror Scan Rate	42 Hz
Field of View	30°
GPS Baselines	≤ 13 nm
GPS PDOP	≤ 3.0
GPS Satellite Constellation	≥ 6
Maximum Returns	Unlimited, but typically not more than 5
Intensity	8-bit
Resolution/Density	Average 4 pulses/m ²
Accuracy	RMSE _z ≤ 15 cm



Leica ALS70 LiDAR sensor

All areas were surveyed with an opposing flight line side-lap of $\geq 50\%$ ($\geq 100\%$ overlap) in order to reduce laser shadowing and increase surface laser painting. To accurately solve for laser point position (geographic coordinates x, y and z), the positional coordinates of the airborne sensor and the attitude of the aircraft were recorded continuously throughout the LiDAR data collection mission. Position of the aircraft was measured twice per second (2 Hz) by an onboard differential GPS unit, and aircraft attitude was measured 200 times per second (200 Hz) as pitch, roll and yaw (heading) from an onboard inertial

³ A full flight acquisition report has also been provided with the Ketchikan LiDAR products.

measurement unit (IMU). To allow for post-processing correction and calibration, aircraft and sensor position and attitude data are indexed by GPS time. Please see Appendix C for GPS separation plots, GPS altitude plots, and PDOP plots.

Digital Imagery

Aerial imagery was collected using Quantum Spatial’s Zeiss/Intergraph Digital Mapping Camera (DMC) (Table 8) mounted in a Piper Navajo. The DMC is a large format digital aerial camera manufactured by Zeiss. The system is gyro-stabilized with forward motion compensation and simultaneously collects panchromatic and multispectral (RGB, NIR) imagery through eight individual camera modules. Four high resolution panchromatic camera modules have a 120mm focal length. Similarly, four multispectral camera modules collect RGB and NIR lower resolution imagery at 25mm focal length. Images are created by stitching together raw data from the 4 panchromatic CCDs, and pan-sharpening the multispectral data to yield Level 3 TIFFs.

Table 8: Camera manufacturer’s specifications

Zeiss/Intergraph DMC	
Focal Length	120 mm
Data Format	RGB NIR
Pixel Size	7.2 µm
Image Size	13,824 x 7,680 pixels
Frame Rate	2.1 seconds
FOV	69.3° cross track x 42° along track

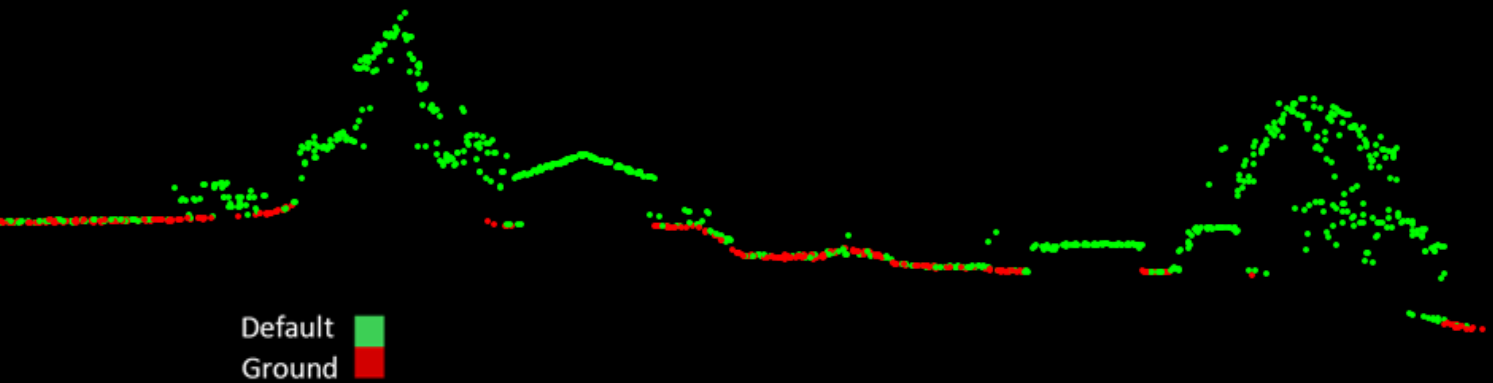


For the Ketchikan site, images were collected in four spectral bands (red, green, blue, and NIR) with 60% along track overlap and 40% sidelap between frames. The acquisition flight parameters were designed to yield a native pixel resolution of ≤ 30 cm. Orthophoto specifications particular to the Ketchikan project are in Table 9.

Table 9: Project-specific orthophoto specifications

Digital Orthophotography Specifications	
Equipment	DMC
Spectral Bands	Red, Green, Blue, NIR
Resolution	4 inch pixel size
Along Track Overlap	≥60%
Flight Altitude (MSL)	2,900 – 4,100 ft
GPS Baselines	≤25 nm
GPS PDOP	≤3.0
GPS Satellite Constellation	≥6
Image	4 band 8-bit GeoTiff

A view of buildings intermixed with vegetation located east of Totem Bight Park. This image was created from a 3 meter cross section and the LiDAR points are colored by classification.



LiDAR Data

Upon completion of data acquisition, QSI processing staff initiated a suite of automated and manual techniques to process the data into the requested deliverables. Processing tasks included GPS control computations, smoothed best estimate trajectory (SBET) calculations, kinematic corrections, calculation of laser point position, sensor and data calibration for optimal relative and absolute accuracy, and LiDAR point classification (Table 10). Processing methodologies were tailored for the landscape. Brief descriptions of these tasks are shown in Table 11.

Table 10: ASPRS LAS classification standards applied to the Ketchikan dataset

Classification Number	Classification Name	Classification Description
1	Default/ Unclassified	Laser returns that are not included in the ground class, composed of vegetation and man-made structures
2	Ground	Laser returns that are determined to be ground using automated and manual cleaning algorithms

Table 11: LiDAR processing workflow

LiDAR Processing Step	Software Used
<p>Resolve kinematic corrections for aircraft position data using kinematic aircraft GPS and static ground GPS data. Develop a smoothed best estimate of trajectory (SBET) file that blends post-processed aircraft position with sensor head position and attitude recorded throughout the survey.</p>	<p>IPAS TC v.3.1 Waypoint Inertial Explorer v.8.5</p>
<p>Calculate laser point position by associating SBET position to each laser point return time, scan angle, intensity, etc. Create raw laser point cloud data for the entire survey in *.las (ASPRS v. 1.2) format. Convert data to orthometric elevations by applying a geoid12a correction.</p>	<p>ALS Post Processing Software v.2.75</p>
<p>Import raw laser points into manageable blocks (less than 500 MB) to perform manual relative accuracy calibration and filter erroneous points. Classify ground points for individual flight lines.</p>	<p>TerraScan v.14</p>
<p>Using ground classified points per each flight line, test the relative accuracy. Perform automated line-to-line calibrations for system attitude parameters (pitch, roll, heading), mirror flex (scale) and GPS/IMU drift. Calculate calibrations on ground classified points from paired flight lines and apply results to all points in a flight line. Use every flight line for relative accuracy calibration.</p>	<p>TerraMatch v.14</p>
<p>Classify resulting data to ground and other client designated ASPRS classifications (Table 10). Assess statistical absolute accuracy via direct comparisons of ground classified points to ground control survey data.</p>	<p>TerraScan v.14 TerraModeler v.14</p>
<p>Generate bare earth models as triangulated surfaces. Generate highest hit models as a surface expression of all classified points. Export all surface models as ESRI GRIDs at a 3.0 foot pixel resolution.</p>	<p>TerraScan v.14 TerraModeler v.14 ArcMap v. 10.1</p>

Feature Extraction

Contours

Contour generation from LiDAR point data required a thinning operation in order to reduce contour sinuosity. The thinning operation reduced point density where topographic change is minimal (i.e., flat surfaces) while preserving resolution where topographic change was present. Model key points were selected from the ground model every 20 feet with the spacing decreased in regions with high surface curvature (Z tolerance of 0.15 feet). Generation of model key points eliminated redundant detail in terrain representation, particularly in areas of low relief, and provided for a more manageable dataset. Contours were produced through TerraModeler by interpolating between the model key points at even elevation increments.

Elevation contour lines were then intersected with ground point density rasters and a confidence field was added to each contour line. Contours which crossed areas of high point density have high confidence levels, while contours which crossed areas of low point density have low confidence levels. Areas with low ground point density are commonly beneath buildings and bridges, in locations with dense vegetation, over water, and in other areas where laser penetration to the ground surface was impeded (Figure 4).

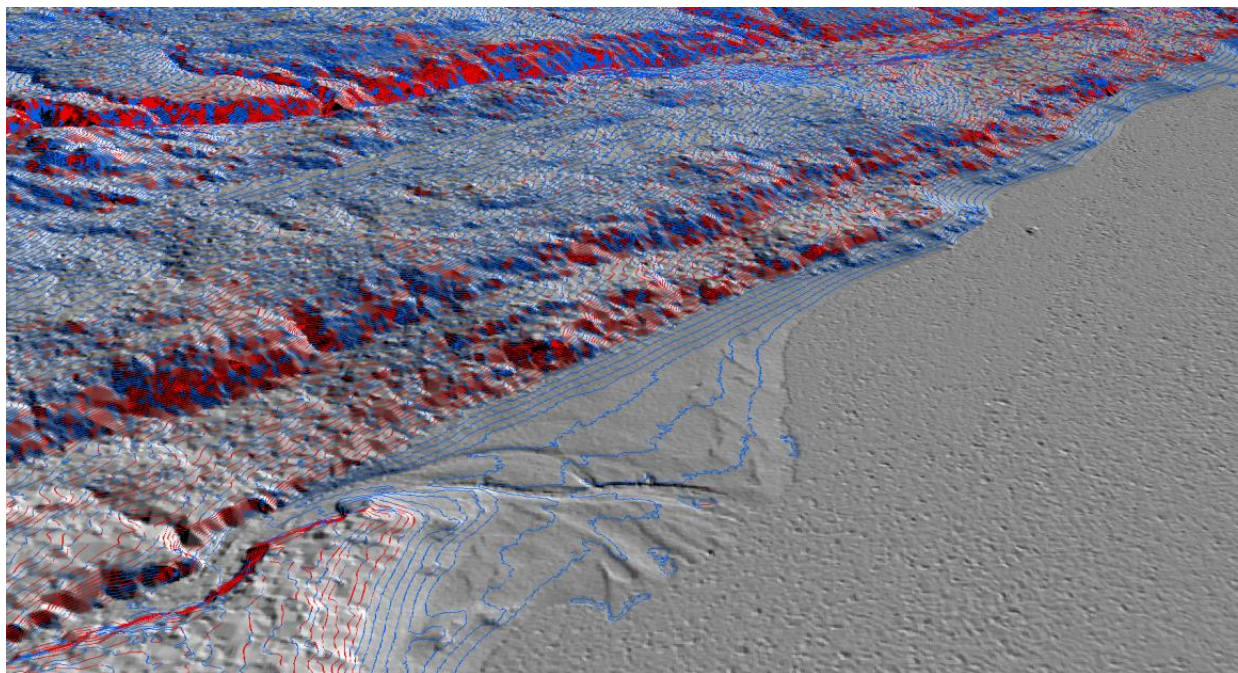


Figure 4: Contours draped over the Ketchikan bare earth elevation model. Blue contours represent high confidence while the red contours represent low confidence.

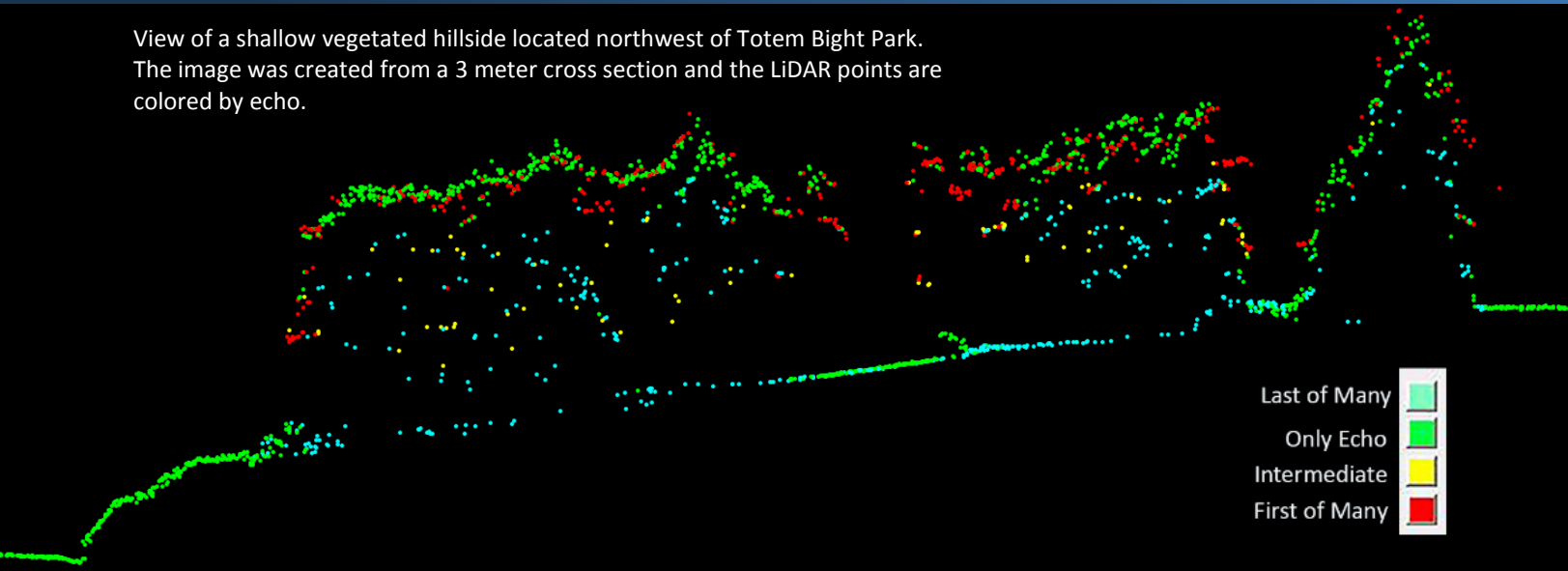
Digital Imagery

The collected digital photographs went through multiple processing steps to create final orthophoto products. Initially, image radiometric values were calibrated to specific gain and exposure settings, and photo position and orientation were calculated by linking the time of image capture to the smoothed best estimate of trajectory (SBET). Within Inpho’s Match-AT, the exterior orientation derived from the SBET was applied to the photo images and the interior orientation of the camera was defined. Adjusted images were orthorectified using the LiDAR-derived Digital Terrain Model (DTM) to remove displacement effects from topographic relief inherent in the imagery. The individual orthorectified TIFFs were mosaicked together using Inpho’s OrthoVista, which adjusted any radiometric differences between images. The processing workflow for orthophotos is summarized in Table 12.

Table 12: Orthophoto processing workflow

Orthophoto Processing Steps	Software Used
Resolve GPS kinematic corrections for the aircraft position data using kinematic aircraft GPS (collected at 2Hz) and static ground GPS (1Hz) data collected over geodetic controls.	POSPac v. 4.4
Develop a smooth best estimate trajectory (SBET) file that blends post-processed aircraft position with attitude data. Sensor heading, position, and attitude are calculated throughout the survey.	POSPac v. 4.4
Create exterior orientation parameters (EO) for each photo image with X, Y, Z, omega, phi, and kappa.	Inpho v. 5.7
Apply EO to photos, measure ground control points and perform aerial triangulation.	Inpho Match-AT v.5.7
Import DTM and orthorectify photos to the specified area of interest.	Inpho OrthoMaster v.5.7
Mosaic orthorectified imagery, blending seams between individual photos and correcting for radiometric differences between photos.	Inpho OrthoVista v. 5.7
Manual image radiometric adjustments	Photoshop CS
GeoTiff projection declared in header	GDAL - Geospatial Data Abstraction Library: Version 1.9.0, Open Source Geospatial Foundation

View of a shallow vegetated hillside located northwest of Totem Bight Park. The image was created from a 3 meter cross section and the LiDAR points are colored by echo.



LiDAR Density

The acquisition parameters were designed to acquire an average first-return density of 4 points/m² (0.37 points/ft²). First return density describes the density of pulses emitted from the laser that return at least one echo to the system. Multiple returns from a single pulse were not considered in first return density analysis. Some types of surfaces (e.g., breaks in terrain, water and steep slopes) may return fewer pulses than originally emitted by the laser. First returns typically reflect off the highest feature on the landscape within the footprint of the pulse. In forested or urban areas the highest feature could be a tree, building or power line, while in areas of unobstructed ground the first return will be the only echo and represents the bare earth surface.

The density of ground-classified LiDAR returns was also analyzed for this project. Terrain character, land cover, and ground surface reflectivity all influenced the density of ground surface returns. In vegetated areas, fewer pulses may penetrate the canopy, resulting in lower ground density.

The average first-return density of LiDAR data for the Ketchikan project was 0.61 points/ft² (6.54 points/m²) while the average ground classified density was 0.09 points/ft² (0.96 points/m²) (Table 13). The statistical and spatial distributions of first return densities and classified ground return densities per 100 m x 100 m cell are portrayed in Figure 5 through Figure 7.

Table 13: Average LiDAR point densities

Classification	Point Density
First-Return	0.61 points/ft ² 6.54 points/m ²
Ground Classified	0.09 points/ft ² 0.96 points/m ²

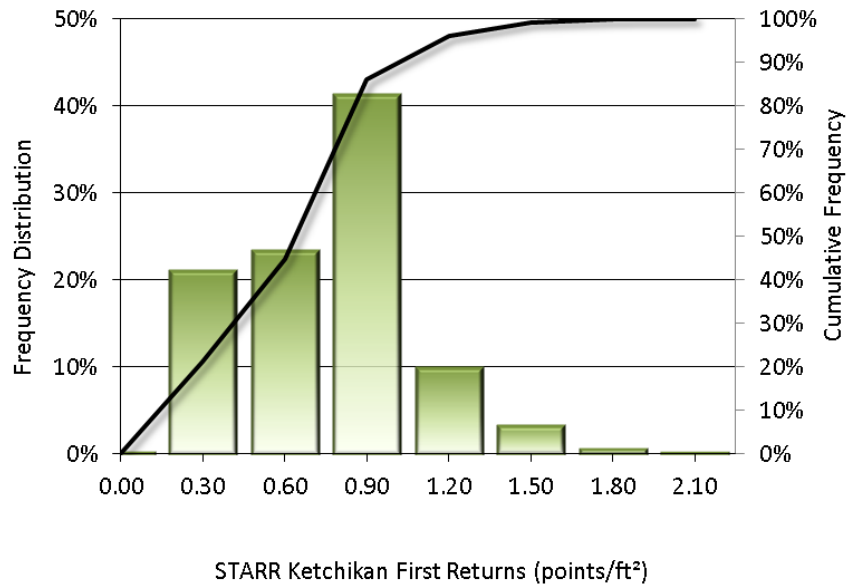


Figure 5: Frequency distribution of first return densities per 100 x 100 m cell

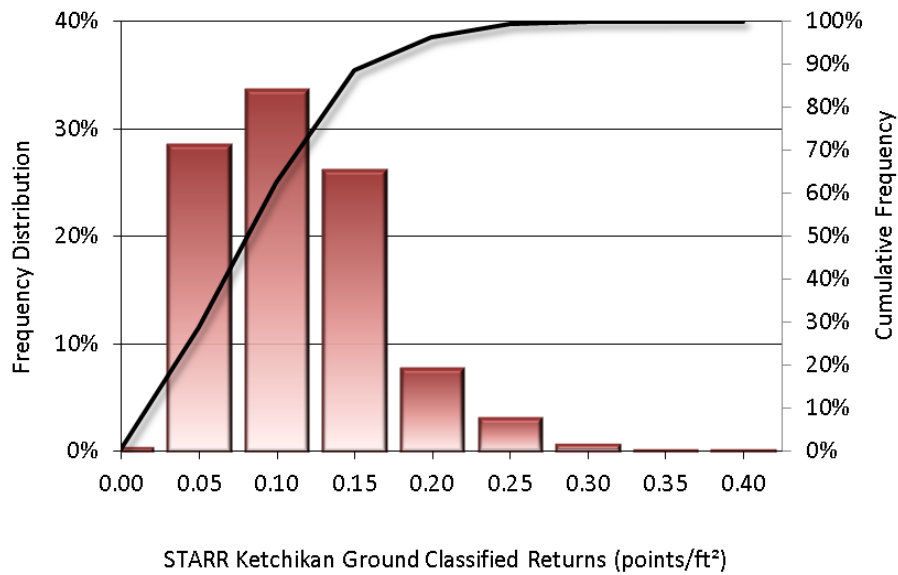


Figure 6: Frequency distribution of ground return densities per 100 x 100 m cell

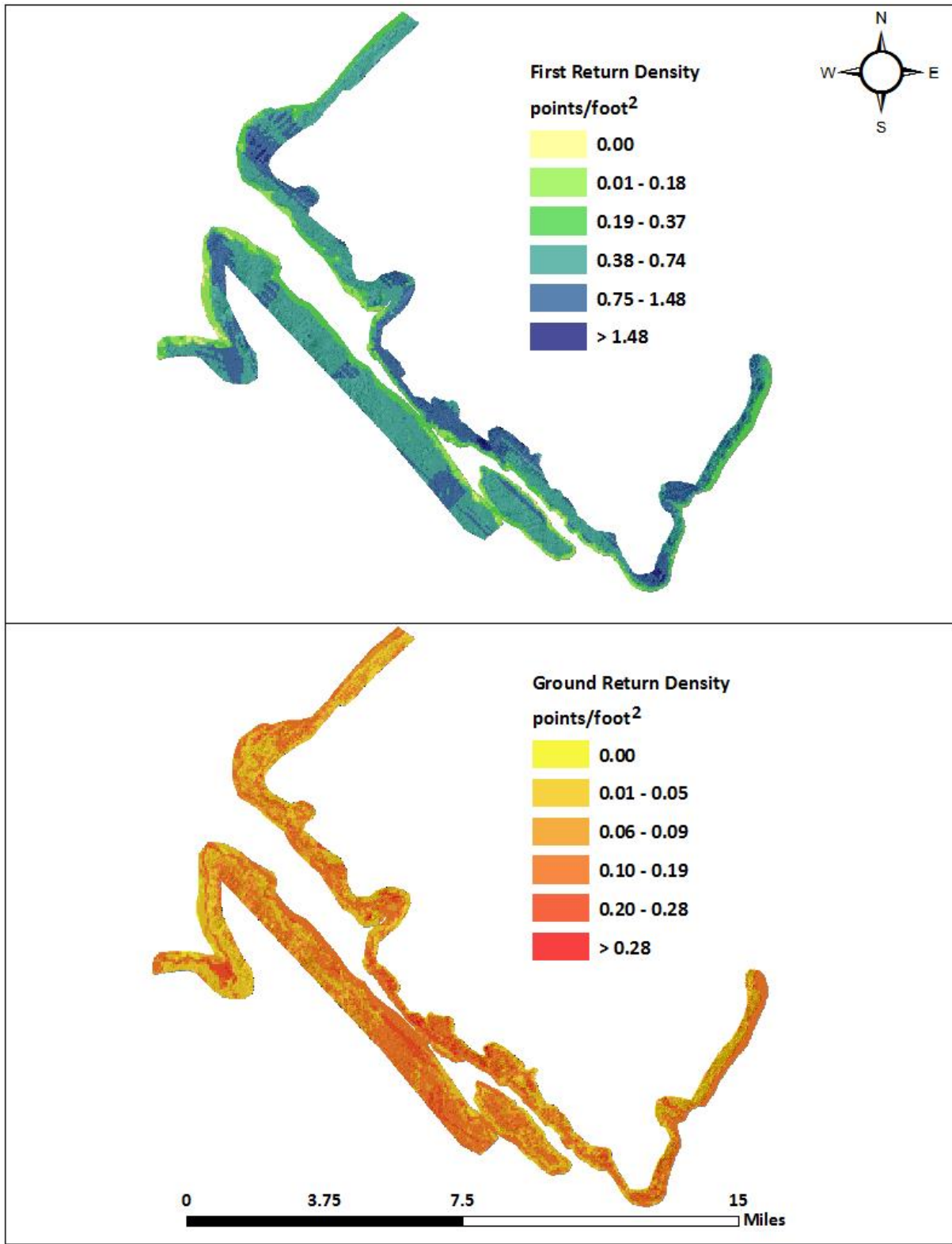


Figure 7: First return and ground density map for the Ketchikan site (100 m x 100 m cells)

LiDAR Accuracy Assessments

The accuracy of the LiDAR data collection can be described in terms of absolute accuracy (the consistency of the data with external data sources) and relative accuracy (the consistency of the dataset with itself). See Appendix A for further information on sources of error and operational measures used to improve relative accuracy.

LiDAR Absolute Accuracy

Absolute accuracy was assessed using Fundamental Vertical Accuracy (FVA) reporting designed to meet guidelines presented in the FGDC National Standard for Spatial Data Accuracy⁴. FVA compares known RTK ground check point data collected on open, bare earth surfaces with level slope (<20°) to the triangulated surface generated by the LiDAR point cloud. FVA is a measure of the accuracy of LiDAR point data in open areas where the LiDAR system has a high probability of measuring the ground surface and is evaluated at the 95% confidence interval (1.96 * RMSE), as shown in Table 14.

The mean and standard deviation (sigma σ) of divergence of the ground surface model from ground survey point coordinates are also considered during accuracy assessment. These statistics assume the error for x, y and z is normally distributed, and therefore the skew and kurtosis of distributions are also considered when evaluating error statistics. For the Ketchikan survey, 20 ground check points were collected in total resulting in a Fundamental Vertical Accuracy of 0.264 feet (0.081 meters), tested as the 95% confidence interval (Figure 8).

Table 14: Absolute accuracy

Absolute Accuracy	
Sample	20 points
FVA (1.96*RMSE)	0.264 ft 0.081 m
Average	0.117 ft 0.036 m
Median	0.136 ft 0.042 m
RMSE	0.135 ft 0.041 m
Standard Deviation (1 σ)	0.069 ft 0.021 m

⁴ Federal Geographic Data Committee, Geospatial Positioning Accuracy Standards (FGDC-STD-007.3-1998). Part 3: National Standard for Spatial Data Accuracy. <http://www.fgdc.gov/standards/projects/FGDC-standards-projects/accuracy/part3/chapter3>

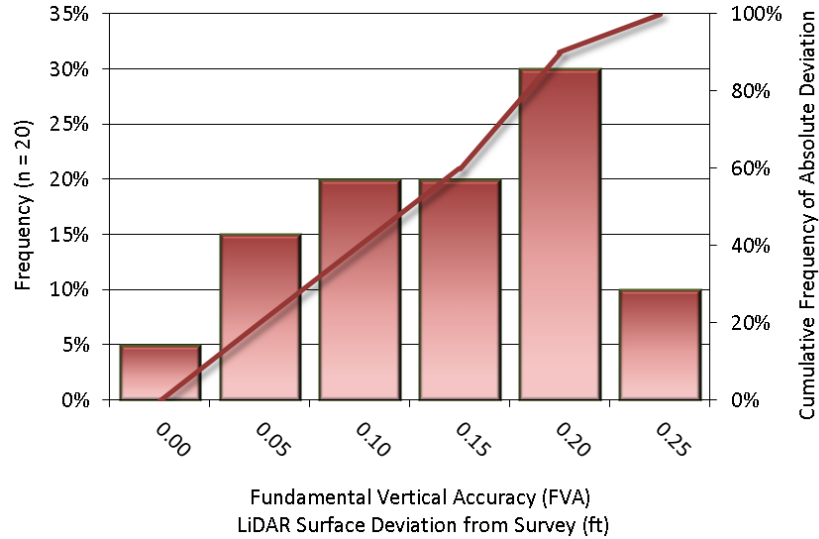


Figure 8: Frequency histogram for LiDAR surface deviation from ground check point values

LiDAR Supplemental and Consolidated Vertical Accuracies

QSI also assessed absolute vertical accuracy using Supplemental Vertical Accuracy (SVA) and Consolidated Vertical Accuracy (CVA) reporting. SVA compares known RTK ground check point data within individual land cover class categories to the triangulated surface generated by the ground classified LiDAR points. CVA, rather, compares known RTK ground check points within all land cover classes to the triangulated surface generated by the ground classified LiDAR points. Both SVA and CVA are evaluated at the 95th percentile (Table 15, Figure 9). Please see Appendix B for frequency histograms for individual land classes.

Table 15: Supplemental and Consolidated Vertical Accuracies

Supplemental and Consolidated Vertical Accuracies				
	SVA			CVA
Land Cover Class	Bare Earth	Urban/Park/Rec	Evergreen Forest	All Land Cover Classes
Sample	20 points	36 points	37 points	93 points
Average Dz	-0.004 ft	0.051 ft	-0.086 ft	-0.015 ft
	-0.001 m	0.016 m	-0.026 m	-0.005 m
Median	-0.003 ft	0.072 ft	-0.079 ft	0.000 ft
	-0.001 m	0.022 m	-0.024 m	0.000 m
RMSE	0.069 ft	0.088 ft	0.219 ft	0.152 ft
	0.021 m	0.027 m	0.067 m	0.046 m
Standard Deviation (1σ)	0.070 ft	0.073 ft	0.204 ft	0.152 ft
	0.021 m	0.022 m	0.062 m	0.046 m
95 th Percentile	0.119 ft	0.151 ft	0.403 ft	0.150 ft
	0.036 m	0.046 m	0.123 m	0.046 m

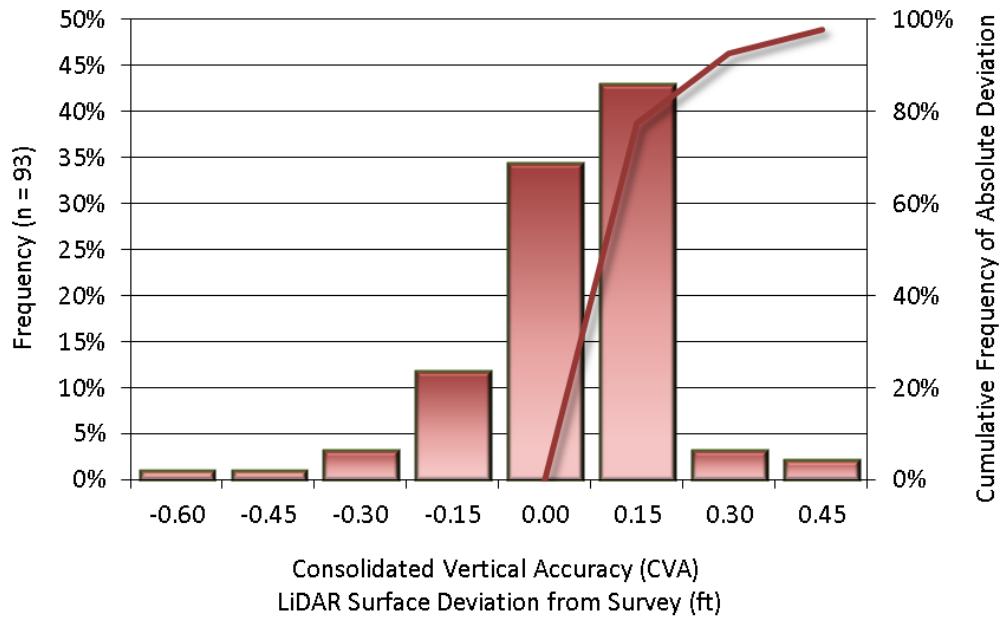


Figure 9: Frequency histogram for LiDAR surface deviation from all land class RTK values

Digital Imagery Accuracy Assessment

Photo-identifiable GPS control and photogrammetric checkpoints were measured and their locations were compared against the orthorectified mosaic using Accuracy Analyst. The displacement was recorded for statistical analysis.

The circular standard error (CSE) for the Ketchikan site was 0.245 ft measured by the ground check points. Circular standard error was approximated based on the FGDC National Standard for Spatial Data Accuracy for horizontal accuracy⁵. The CSE (at 39.35% standard) was computed as follows:

<i>where $RMSE_x = RMSE_y$:</i>	$CSE = 1.7308 * RMSE_{xy}$
<i>where $RMSE_{min}/RMSE_{max}$ is between 0.6-1.0:</i>	$CSE = 0.5 * (RMSE_x + RMSE_y)$
<i>where $RMSE_{min}/RMSE_{max}$ is not between 0.6-1.0:</i>	$CSE = 2.4477 * 0.5 * (RMSE_x + RMSE_y)$
<i>($RMSE_{min/max}$ is the lower/higher value of $RMSE_x$ or $RMSE_y$)</i>	

Table 16 presents the complete photo accuracy statistics, Figure 10 contains a scatterplot showing congruence between orthophoto candidate pixels and ground target locations, and Figure 11 shows an example of the co-registration of the orthophotos to the ground target locations.⁶

⁵ Federal Geographic Data Committee, Geospatial Positioning Accuracy Standards (FGDC-STD-007.3-1998). Part 3: National Standard for Spatial Data Accuracy, Appendix 3-A, page 3-10. <http://www.fgdc.gov/standards/projects/FGDC-standards-projects/accuracy/part3/chapter3>

⁶ A full orthophotography accuracy report has been provided with the STARR Ketchikan products.

Table 16: Orthophotography accuracy statistics for Ketchikan

Min ΔX :	-0.239
Min ΔY :	-0.195
Max ΔX :	0.282
Max ΔY :	0.369
Mean ΔX :	0.023
Mean ΔY :	0.022
RmseX:	0.095
RmseY:	0.105
RmseH:	0.141
NSSDA:	0.245
No. Obs.:	114
CE 90:	0.21
CE 95:	0.239
CI:	0.018

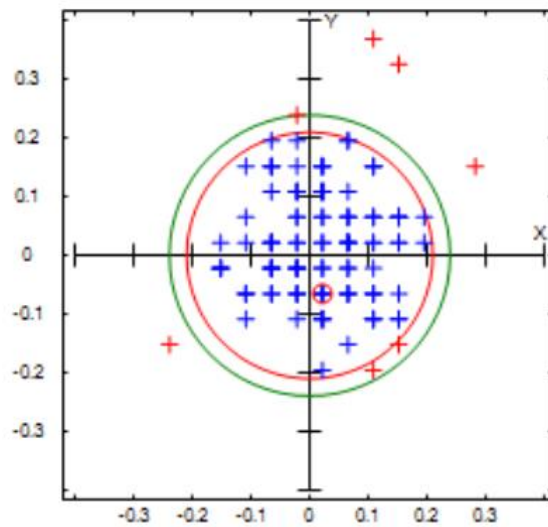


Figure 10: Scatterplot displaying the XY deviation of ground check points aligned with the orthophoto imagery.

Point 302:

X1: 3093121.096 Y1: 1292528.995 X2: 3093121.205 Y2: 1292529.06 Delta X: 0.109 Delta Y: 0.065



Figure 11: Image displaying the co-registration of a GPS ground check point and the rectified imagery in the Ketchikan site.

CERTIFICATIONS

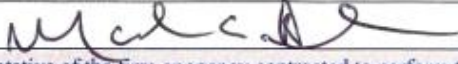
Project Name:	STARR Ketchikan LiDAR & Imagery
Statement of Work No.:	<u>FEMA Task Order: HSFE10-13-J-0073</u>
Interagency Agreement No.:	<u>N/A</u>
CTP Agreement No.:	<u>STARR Partner Tracking #: QS 10 09 001</u>
Statement/Agreement Date:	<u>6/1/14</u>
Certification Date:	<u>9/25/14</u>
Tasks/Activities Covered by This Certification (Check All That Apply)	
<input type="checkbox"/>	Base Map
<input checked="" type="checkbox"/>	Topographic Data Development
<input checked="" type="checkbox"/>	Survey
<input type="checkbox"/>	Hydrologic Analysis
<input type="checkbox"/>	Hydraulic Analysis
<input type="checkbox"/>	Alluvial Fan Analysis
<input type="checkbox"/>	Coastal Analysis
<input type="checkbox"/>	Floodplain Mapping
<p>This is to certify that the work summarized above was completed in accordance with the statement/agreement cited above and all amendments thereto, together with all such modifications, either written or oral, as the Regional Project Officer and/or Assistance Officer or their representative have directed, as such modifications affect the statement/agreement, and that all such work has been accomplished in accordance with the provisions contained in <i>Guidelines and Specifications for Flood Hazard Mapping Partners</i> cited in the contract document, and in accordance with sound and accepted engineering practices within the contract provisions for respective phases of the work. This is also to certify that data files submitted for the work summarized above are complete and final. Any revisions made to the already submitted data are included in the final submittal.</p>	
Name:	MARK E MEADE
Title:	SR VICE PRESIDENT
Firm/Agency Represented:	QUANTUM SPATIAL
Registration No.:	KY PE 15056 CPR1050
Signature:	
<p>This form must be signed by a representative of the firm or agency contracted to perform the work, who must be a registered or certified professional in the area of work performed, in compliance with Federal and State regulations.</p>	



Figure 12: A view looking North over Pennock Island. The image was created from the gridded LiDAR surface colored by elevation.



Figure 13: View looking Northeast over Ketchikan, Alaska. The image was created from the orthoimagery draped over the gridded LiDAR surface and overlaid with the LiDAR point cloud.

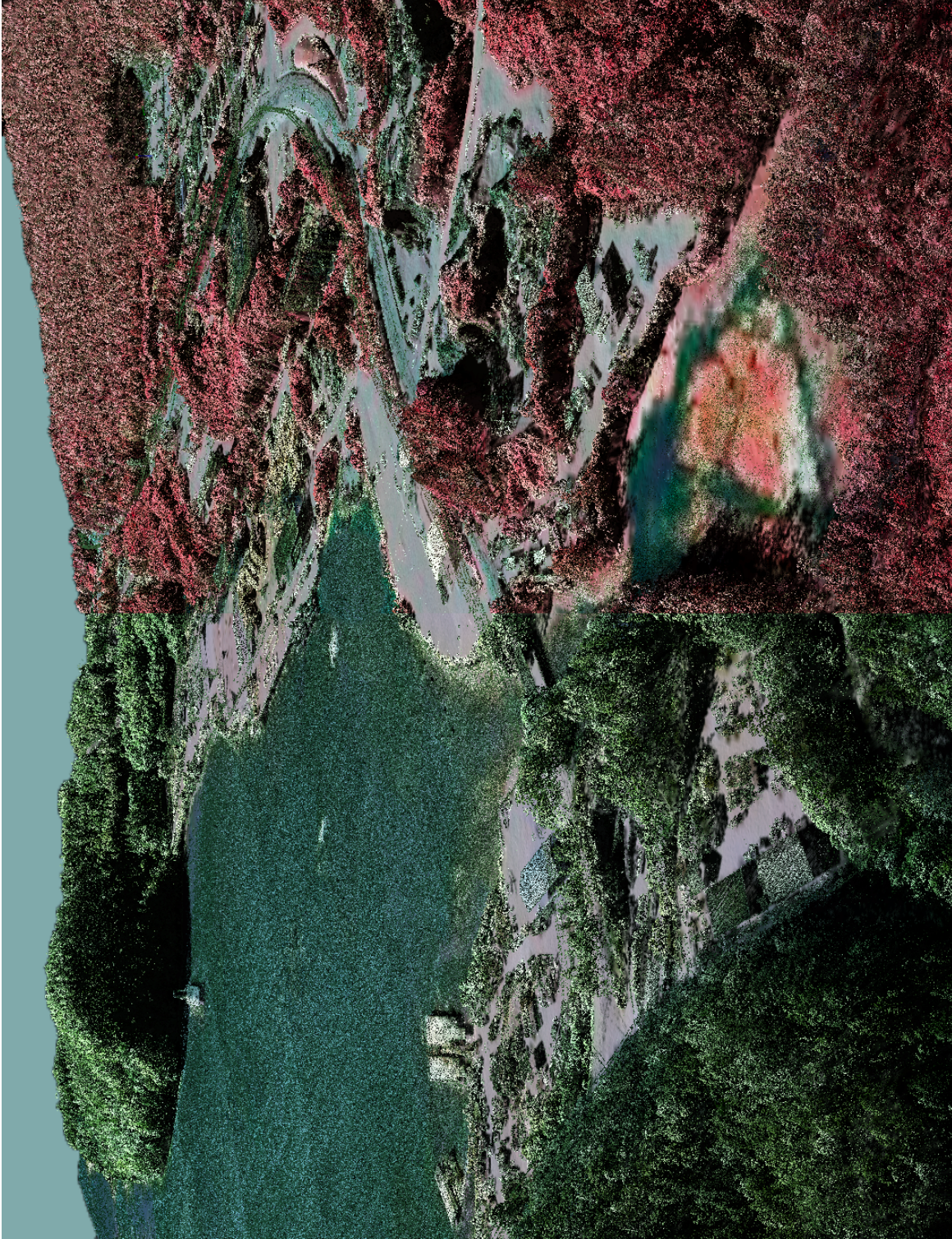


Figure 14: A view looking west over Ward Cove, Alaska. The image was created from the orthoimagery (RGB on left, CIR on right) draped over the gridded LiDAR surface and overlaid with the LiDAR point cloud.

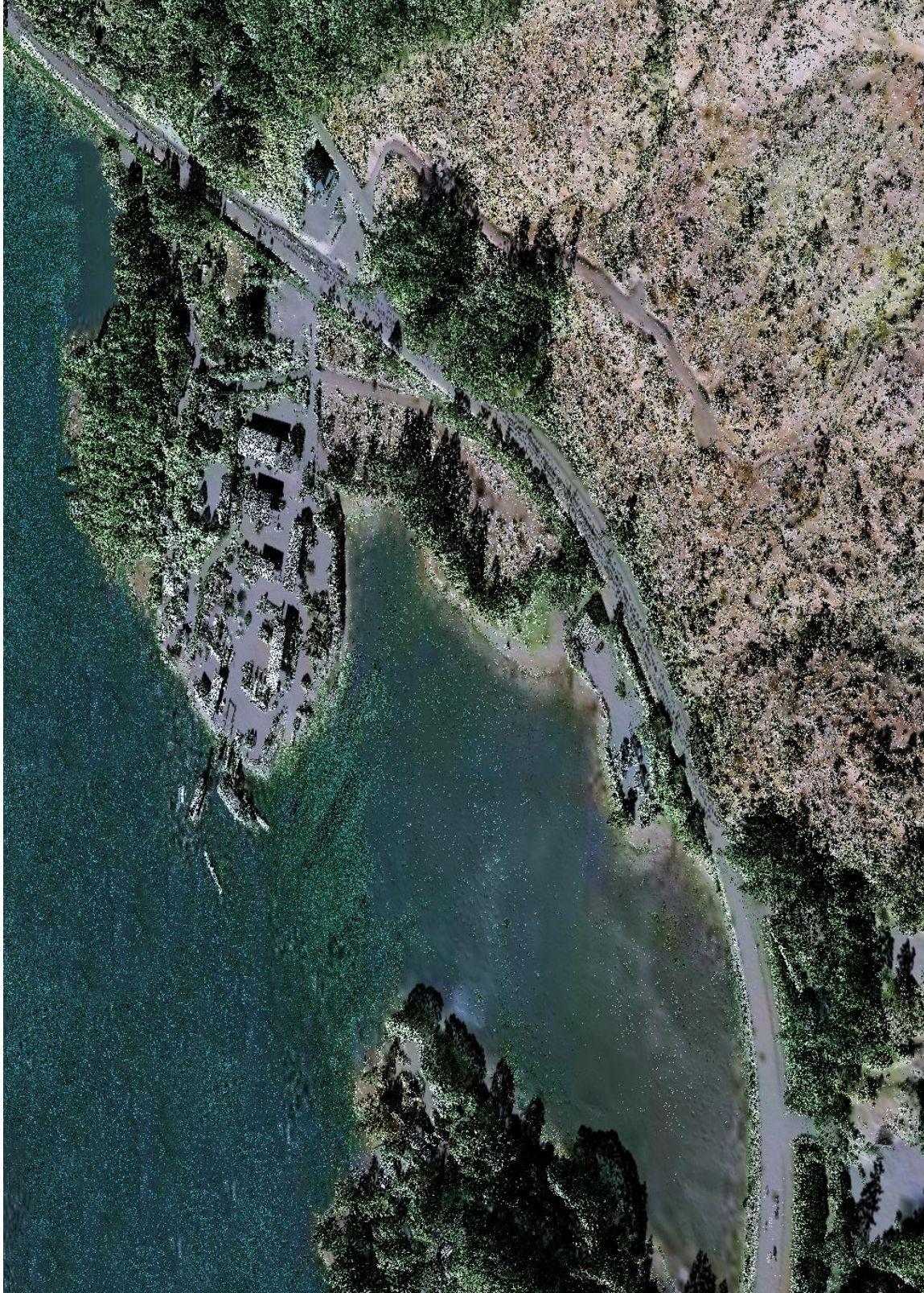


Figure 15: View looking West over the North Tongass Highway traveling through Totem Bight State Park. The image was created from the orthoimagery draped over the gridded LiDAR surface colored by elevation and overlaid with the LiDAR point cloud.

1-sigma (σ) Absolute Deviation: Value for which the data are within one standard deviation (approximately 68th percentile) of a normally distributed data set.

1.96 * RMSE Absolute Deviation: Value for which the data are within two standard deviations (approximately 95th percentile) of a normally distributed data set, based on the FGDC standards for Fundamental Vertical Accuracy (FVA) reporting.

Accuracy: The statistical comparison between known (surveyed) points and laser points. Typically measured as the standard deviation (σ) and root mean square error (RMSE).

Absolute Accuracy: The vertical accuracy of LiDAR data is described as the mean and standard deviation (σ) of divergence of LiDAR point coordinates from ground survey point coordinates. To provide a sense of the model predictive power of the dataset, the root mean square error (RMSE) for vertical accuracy is also provided. These statistics assume the error distributions for x, y and z are normally distributed, and thus we also consider the skew and kurtosis of distributions when evaluating error statistics.

Relative Accuracy: Relative accuracy refers to the internal consistency of the data set; i.e., the ability to place a laser point in the same location over multiple flight lines, GPS conditions and aircraft attitudes. Affected by system attitude offsets, scale and GPS/IMU drift, internal consistency is measured as the divergence between points from different flight lines within an overlapping area. Divergence is most apparent when flight lines are opposing. When the LiDAR system is well calibrated, the line-to-line divergence is low (<10 cm).

Root Mean Square Error (RMSE): A statistic used to approximate the difference between real-world points and the LiDAR points. It is calculated by squaring all the values, then taking the average of the squares and taking the square root of the average.

Data Density: A common measure of LiDAR resolution, measured as points per square meter.

Digital Elevation Model (DEM): File or database made from surveyed points, containing elevation points over a contiguous area. Digital terrain models (DTM) and digital surface models (DSM) are types of DEMs. DTMs consist solely of the bare earth surface (ground points), while DSMs include information about all surfaces, including vegetation and man-made structures.

Intensity Values: The peak power ratio of the laser return to the emitted laser, calculated as a function of surface reflectivity.

Nadir: A single point or locus of points on the surface of the earth directly below a sensor as it progresses along its flight line.

Overlap: The area shared between flight lines, typically measured in percent. 100% overlap is essential to ensure complete coverage and reduce laser shadows.

Pulse Rate (PR): The rate at which laser pulses are emitted from the sensor; typically measured in thousands of pulses per second (kHz).

Pulse Returns: For every laser pulse emitted, the number of wave forms (i.e., echos) reflected back to the sensor. Portions of the wave form that return first are the highest element in multi-tiered surfaces such as vegetation. Portions of the wave form that return last are the lowest element in multi-tiered surfaces.

Real-Time Kinematic (RTK) Survey: A type of surveying conducted with a GPS base station deployed over a known monument with a radio connection to a GPS rover. Both the base station and rover receive differential GPS data and the baseline correction is solved between the two. This type of ground survey is accurate to 1.5 cm or less.

Post-Processed Kinematic (PPK) Survey: GPS surveying is conducted with a GPS rover collecting concurrently with a GPS base station set up over a known monument. Differential corrections and precisions for the GNSS baselines are computed and applied after the fact during processing. This type of ground survey is accurate to 1.5 cm or less.

Scan Angle: The angle from nadir to the edge of the scan, measured in degrees. Laser point accuracy typically decreases as scan angles increase.

Native LiDAR Density: The number of pulses emitted by the LiDAR system, commonly expressed as pulses per square meter.

APPENDIX A - ACCURACY CONTROLS

Relative Accuracy Calibration Methodology:

Manual System Calibration: Calibration procedures for each mission require solving geometric relationships that relate measured swath-to-swath deviations to misalignments of system attitude parameters. Corrected scale, pitch, roll and heading offsets were calculated and applied to resolve misalignments. The raw divergence between lines was computed after the manual calibration was completed and reported for each survey area.

Automated Attitude Calibration: All data were tested and calibrated using TerraMatch automated sampling routines. Ground points were classified for each individual flight line and used for line-to-line testing. System misalignment offsets (pitch, roll and heading) and scale were solved for each individual mission and applied to respective mission datasets. The data from each mission were then blended when imported together to form the entire area of interest.

Automated Z Calibration: Ground points per line were used to calculate the vertical divergence between lines caused by vertical GPS drift. Automated Z calibration was the final step employed for relative accuracy calibration.

LiDAR accuracy error sources and solutions:

Type of Error	Source	Post Processing Solution
GPS (Static/Kinematic)	Long Base Lines	None
	Poor Satellite Constellation	None
	Poor Antenna Visibility	Reduce Visibility Mask
Relative Accuracy	Poor System Calibration	Recalibrate IMU and sensor offsets/settings
	Inaccurate System	None
Laser Noise	Poor Laser Timing	None
	Poor Laser Reception	None
	Poor Laser Power	None
	Irregular Laser Shape	None

Operational measures taken to improve relative accuracy:

Low Flight Altitude: Terrain following was employed to maintain a constant above ground level (AGL). Laser horizontal errors are a function of flight altitude above ground (about 1/3000th AGL flight altitude).

Focus Laser Power at narrow beam footprint: A laser return must be received by the system above a power threshold to accurately record a measurement. The strength of the laser return (i.e., intensity) is a function of laser emission power, laser footprint, flight altitude and the reflectivity of the target. While surface reflectivity cannot be controlled, laser power can be increased and low flight altitudes can be maintained.

Reduced Scan Angle: Edge-of-scan data can become inaccurate. The scan angle was reduced to a maximum of $\pm 15^\circ$ from nadir, creating a narrow swath width and greatly reducing laser shadows from trees and buildings.

Quality GPS: Flights took place during optimal GPS conditions (e.g., 6 or more satellites and PDOP [Position Dilution of Precision] less than 3.0). Before each flight, the PDOP was determined for the survey day. During all flight times, a dual frequency DGPS base station recording at 1 second epochs was utilized and a maximum baseline length between the aircraft and the control points was less than 13 nm at all times.

Ground Survey: Ground survey point accuracy (<1.5 cm RMSE) occurs during optimal PDOP ranges and targets a minimal baseline distance of 4 miles between GPS rover and base. Robust statistics are, in part, a function of sample size (n) and distribution. Ground survey points are distributed to the extent possible throughout multiple flight lines and across the survey area.

50% Side-Lap (100% Overlap): Overlapping areas are optimized for relative accuracy testing. Laser shadowing is minimized to help increase target acquisition from multiple scan angles. Ideally, with a 50% side-lap, the nadir portion of one flight line coincides with the swath edge portion of overlapping flight lines. A minimum of 50% side-lap with terrain-followed acquisition prevents data gaps.

Opposing Flight Lines: All overlapping flight lines have opposing directions. Pitch, roll and heading errors are amplified by a factor of two relative to the adjacent flight line(s), making misalignments easier to detect and resolve.

LiDAR Supplemental Vertical Accuracies

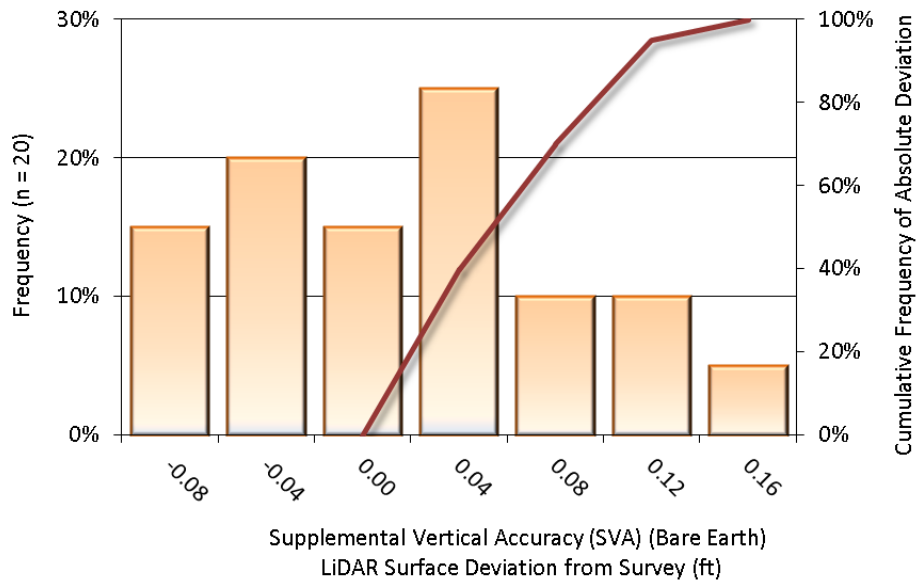


Figure 16: Frequency histogram for LiDAR surface deviation from "Bare Earth" land class RTK values

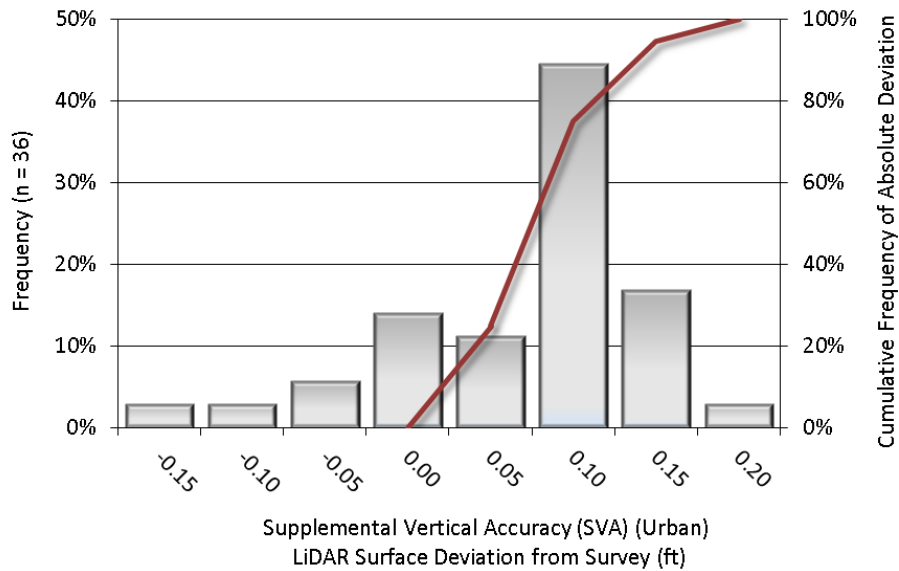


Figure 17: Frequency histogram for LiDAR surface deviation from "Urban/Park/Rec" land class RTK values

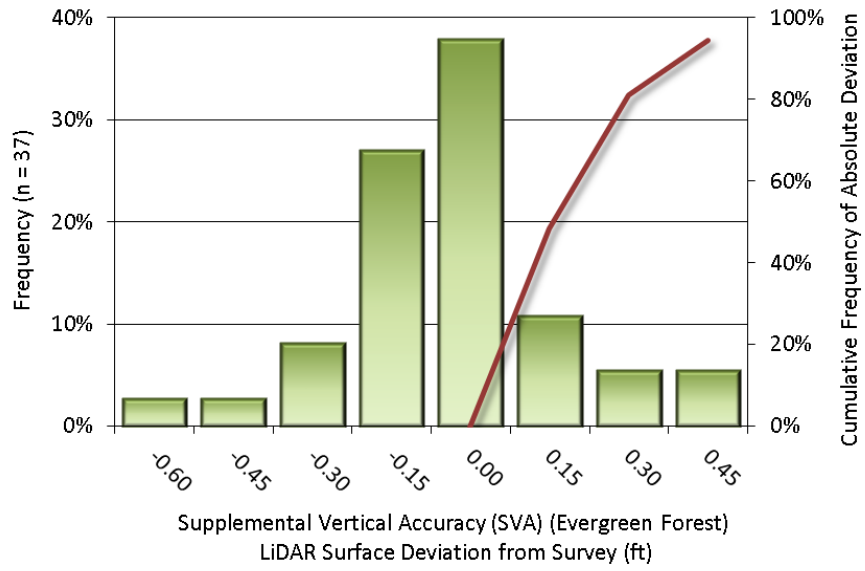


Figure 18: Frequency histogram for LiDAR surface deviation from “Evergreen Forest” land class RTK values

GPS Separation and Altitude Plots, PDOP Plots

07/12/2014

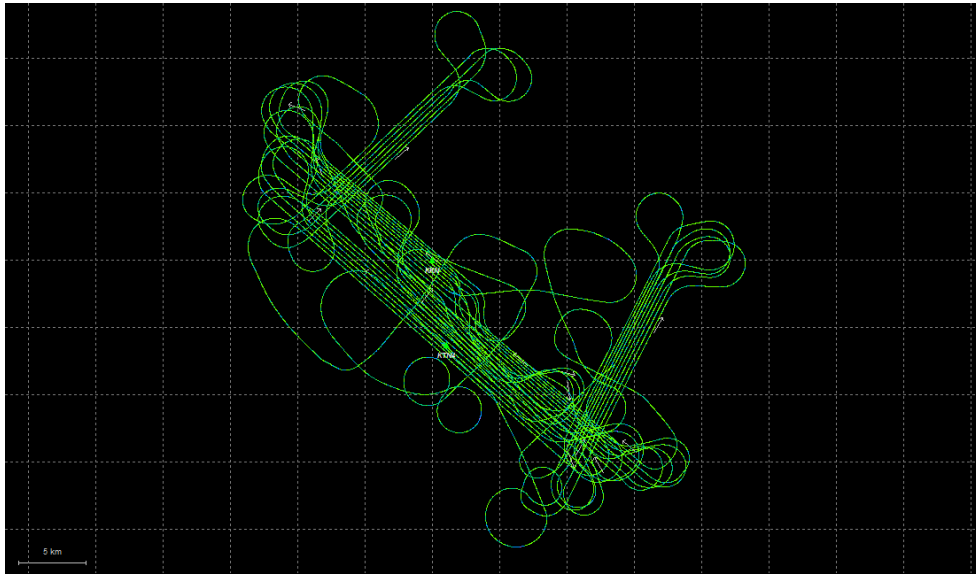


Figure 19: Map of the Smoothed Best Estimate of Trajectory for STARR Ketchikan LiDAR, 07/12/2014

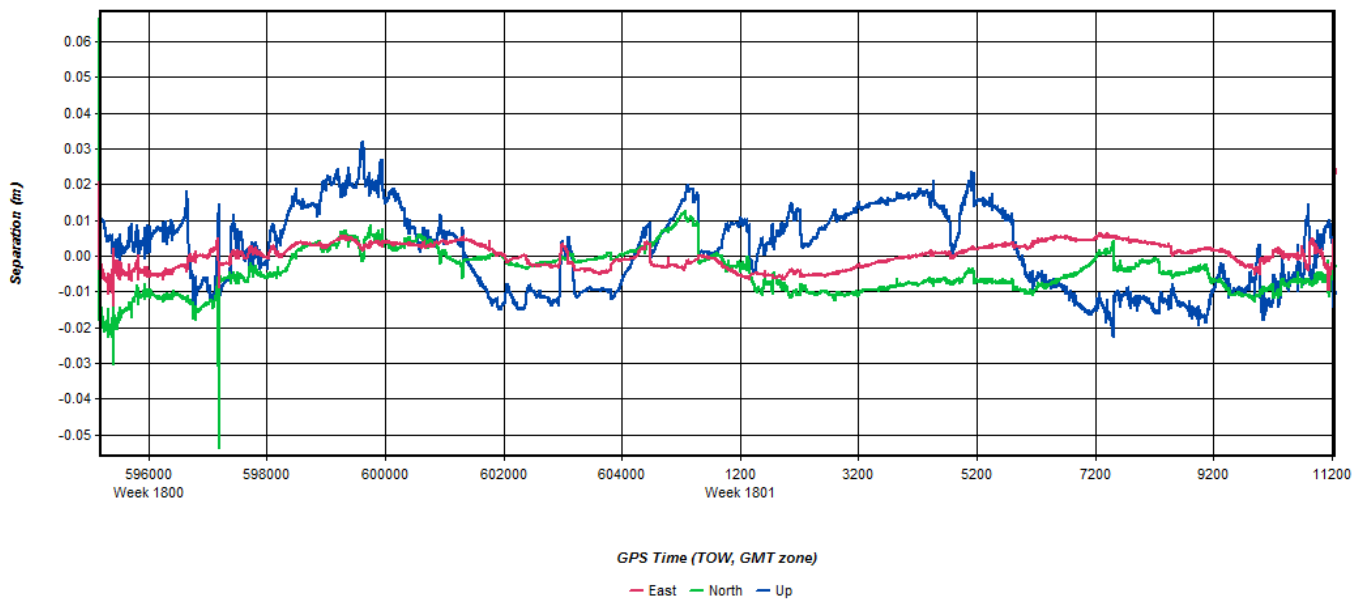


Figure 20: Combined Separation Plot for STARR Ketchikan LiDAR, 07/12/2014

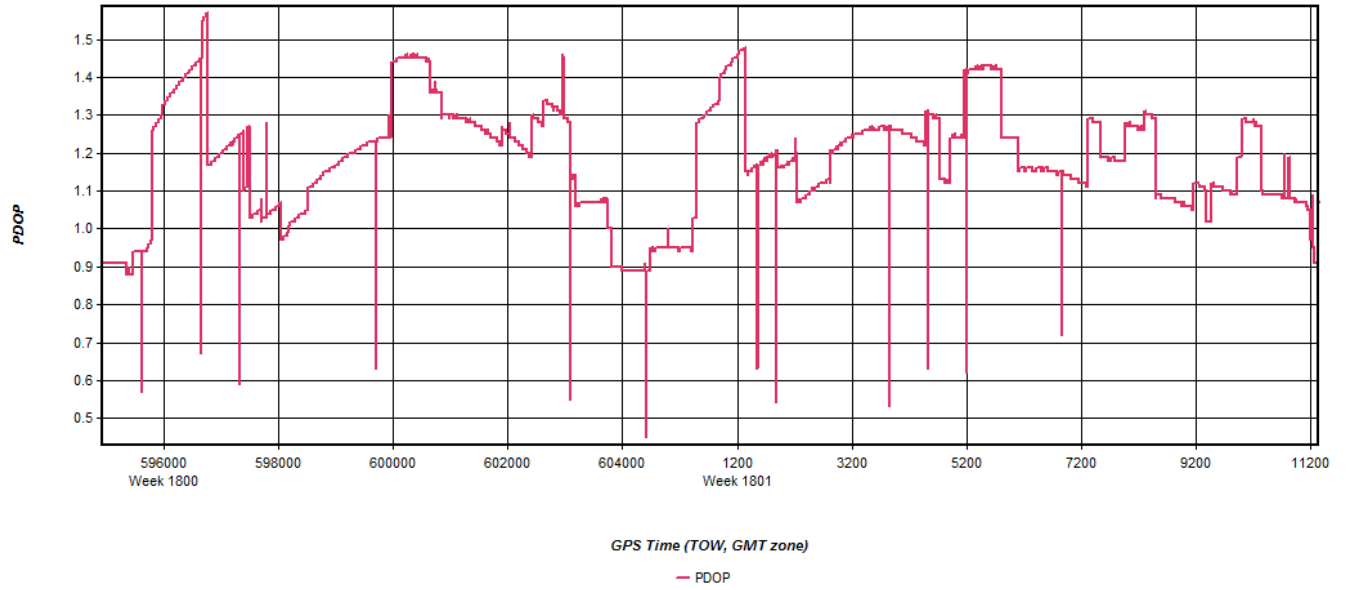


Figure 21: STARR Ketchikan LIDAR, Position Dilution of Precision plot, 07/12/2014

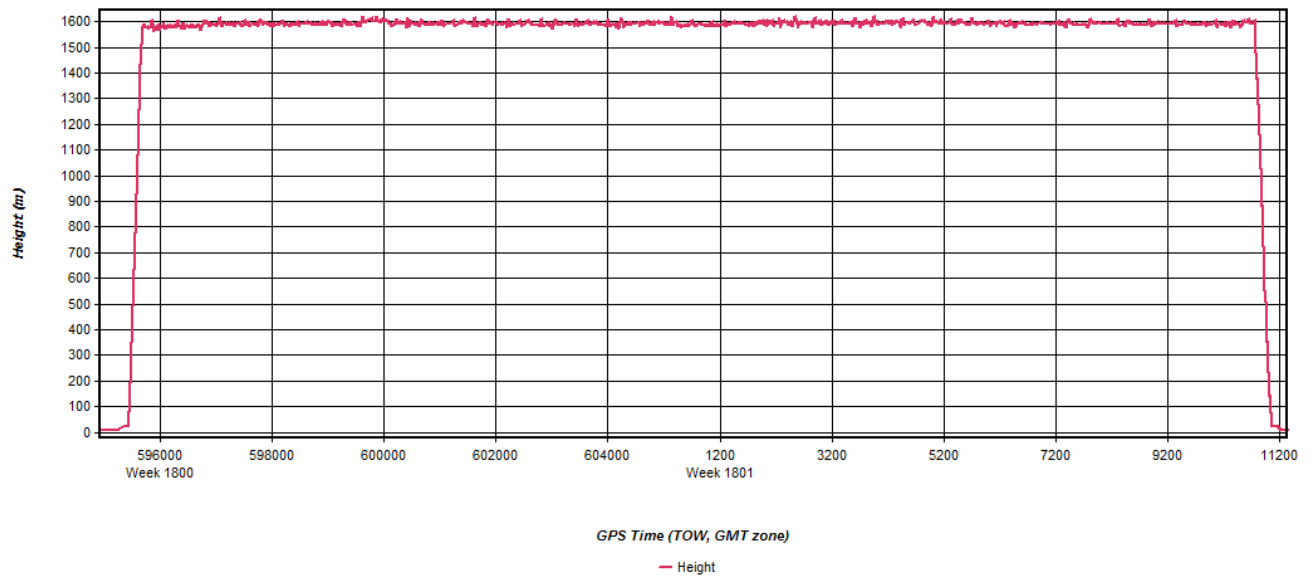


Figure 22: Height profile plot, STARR Ketchikan LiDAR, 07/12/2014

07/13/2014

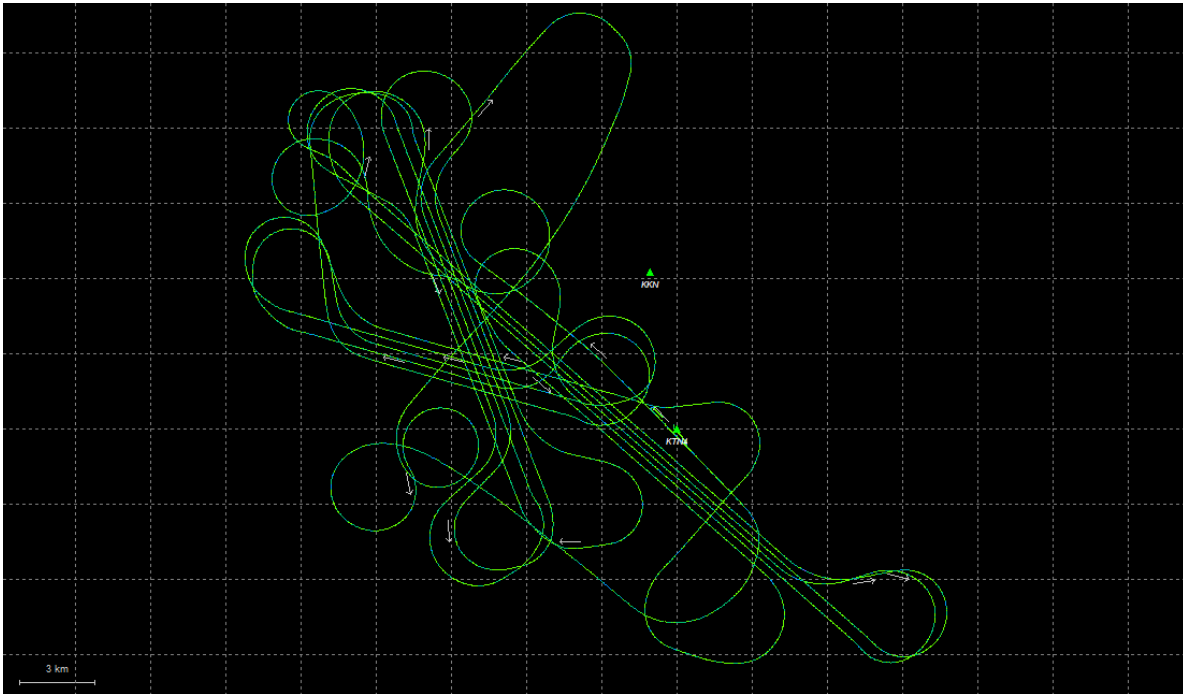


Figure 23: Map of the Smoothed Best Estimate of Trajectory for STARR Ketchikan LiDAR, 07/13/2014



Figure 24: Combined Separation Plot for STARR Ketchikan LiDAR, 07/13/2014

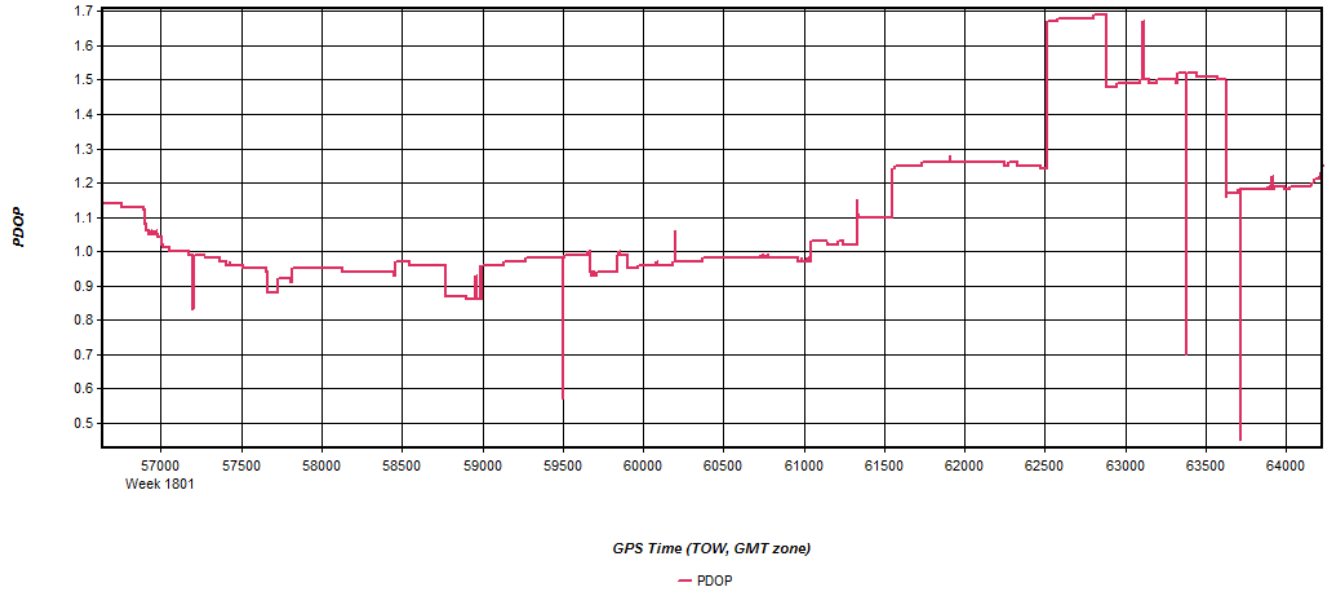


Figure 25: STARR Ketchikan LIDAR, Position Dilution of Precision plot, 07/13/2014

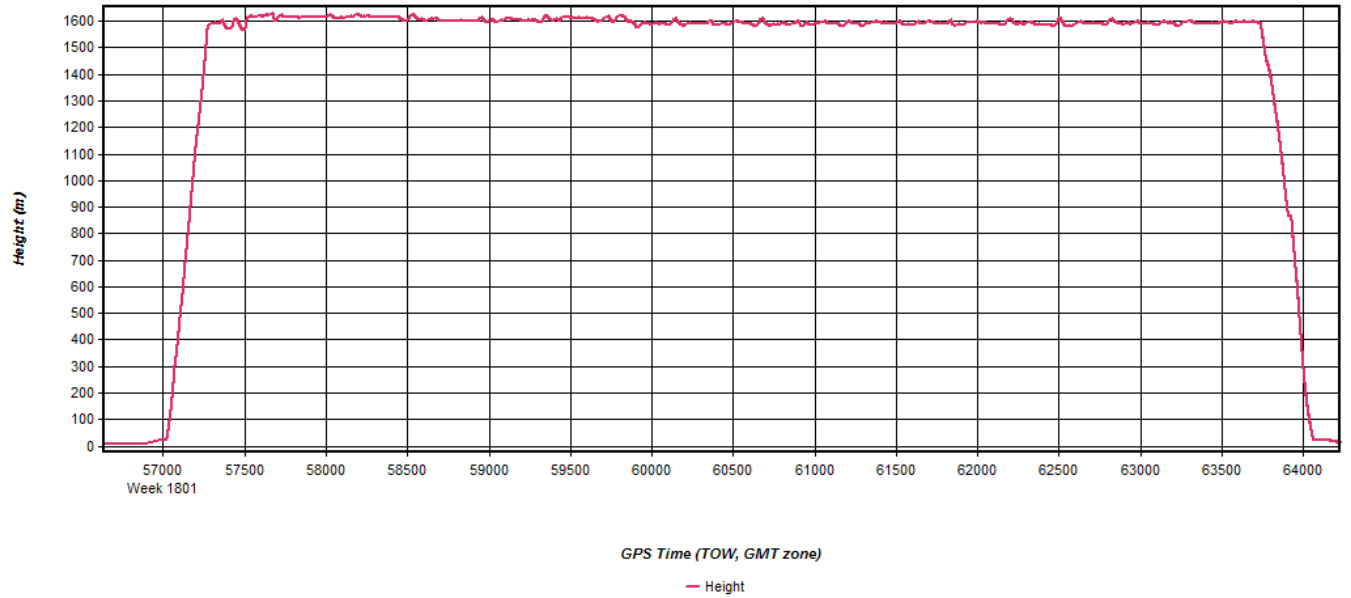


Figure 26: Height profile plot, STARR Ketchikan LiDAR, 07/13/2014